

ARTICLES

Exchange Interaction in Radical–Triplet Pairs: Evidences for CIDEP Generation by Level Crossings in Triplet–Doublet Interactions

Yasuhiro Kobori,[†] Keizo Takeda, Kazuhide Tsuji, Akio Kawai, and Kinichi Obi*[‡]

Department of Chemistry, Tokyo Institute of Technology, Ohokayama, Meguro, Tokyo 152, Japan

Received: January 23, 1998; In Final Form: April 16, 1998

Chemically induced dynamic electron polarization (CIDEP) generated through interaction of the excited triplet state of 1-chloronaphthalene, benzophenone, benzil, and Buckminsterfullerene (C_{60}) with 2,2,6,6-tetramethyl-1-piperidinyloxy (TEMPO) radical was investigated by using time-resolved ESR spectroscopy. We carefully examined what factors affect the CIDEP intensities. By comparing CIDEP intensities of TEMPO in the 1-chloronaphthalene, benzophenone, and benzil systems with that obtained in the C_{60} –TEMPO system, the absolute magnitude of net emissive polarization was determined to be -2.2 , -6.9 , and -8.0 , respectively, in the units of Boltzmann polarization. In the 1-chloronaphthalene–TEMPO system, the viscosity effect on the magnitude of net polarization was studied by changing the temperature (226–275 K) in 2-propanol. The emissive polarization was concluded to result from the state mixing between quartet and doublet manifolds in a radical–triplet pair induced by the zero-field splitting interaction of the counter triplet molecule. The magnitude of net polarization is much larger than the polarization calculated with the reported theory that the CIDEP is predominantly generated in the region where the exchange interaction is smaller than the Zeeman energy. Our experimental results are quantitatively explained by the theory that the CIDEP is generated predominantly in the regions where the quartet and doublet levels cross. We propose a theoretical treatment to calculate the magnitude of net polarization generated by the level crossings in the radical–triplet pair mechanism under highly viscous conditions and perform a numerical analysis of the net RTPM polarization with the stochastic-Liouville equation. The viscosity dependence of the net polarization indicates that the back transition from the doublet to quartet states sufficiently occurs in the level-crossing region under highly viscous conditions. The estimated large exchange interaction suggests that the quenching of the excited triplet molecules by TEMPO proceeds via the electron exchange interaction.

1. Introduction

The quenching of the electronically excited molecules by paramagnetic species has been extensively studied in many photochemical processes.^{1–8} Specifically, the quenching of the lowest excited triplet state by free radicals was widely investigated with optical spectroscopy. Porter and his co-workers² investigated the quenching of the excited triplet state of aromatic molecules with nitroxyl radicals by using the transient absorption technique, and the quenching rate constants were measured. From the triplet energy dependence of the quenching rate constant, they suggested that charge-transfer (CT) interaction would be dominant for the quenching process. However, the CT mechanism could not explain the experimental result that the solvent polarity did not affect the rate constant of triplet quenching.^{3,4,6}

Recent experiments show that chemically induced dynamic electron polarization (CIDEP) is generated through interactions between excited molecules and free radicals.^{9–17} This phe-

nomenon is explained by magnetic interaction acting on the potential surfaces of spin states of radical–triplet pairs (Figure 1)^{10–21} and is interpreted in terms of the radical–triplet pair mechanism (RTPM). According to RTPM, two patterns of CIDEP are observed on free radicals; one is net emission (E) with an E/A (emission/absorption) pattern (E^*/A pattern) attributed as quartet precursor RTPM (QP-RTPM),^{11–13} and the other is an A^*/E pattern as doublet precursor RTPM (DP-RTPM).^{12,16} In QP-RTPM, triplet molecules are selectively quenched through the doublet spin states of radical–triplet pairs. During the triplet–doublet interaction, the quartet and doublet spin states mix with each other by zero-field splitting (zfs) interaction of the triplet molecule and hyperfine interactions of both species.^{10–21} As a result, E^*/A polarization is generated on radicals. On the other hand, in DP-RTPM, S_1 – T_1 enhanced intersystem crossing caused by radicals selectively yields the doublet spin states of radical–triplet pairs, and hence one observes A^*/E type CIDEP on free radicals.^{12,16}

In the last few years, as for the net polarization in RTPM, spin dynamics in the radical–triplet pair system has been theoretically treated by the stochastic-Liouville equation (SLE).^{14,16–21} Comparing to the spin dynamics in the radical pair mechanism (RPM),^{25–27} spin dynamics in RTPM has been

[†] Present address: Institute for Chemical Reaction Science, Tohoku University, Katahira 2-1-1, Aobaku, Sendai 980-8577, Japan.

[‡] Present address: Department of Chemical and Biological Sciences, Japan Women's University, Mejirodai, Bunkyo-ku, Tokyo 112-8681, Japan.

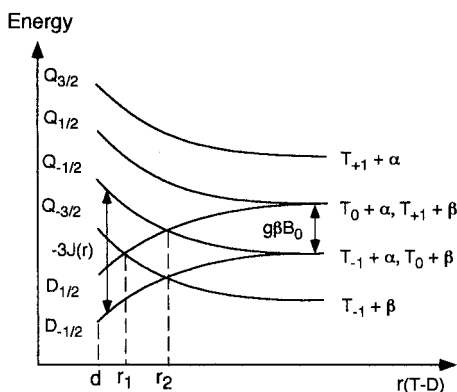


Figure 1. Potential energy surface of spin states in radical–triplet pair with $J < 0$.

considered to be rather complex, and the SLE must be carefully treated. Two types of CIDEP theories are proposed by the use of SLE for the net polarization in RTPM: the mechanisms where the electron exchange interaction (J) in the pair is smaller and much larger than the Zeeman splitting.^{14,16–21} In the former mechanism, the net polarization is generated on free radicals by the quartet–doublet spin relaxation induced through zero-field splitting (zfs) interaction of the excited triplet molecule in regions where the exchange interaction is smaller than the Zeeman energy ($r > r_1, r_2$ in Figure 1).^{14,19,20} In the latter, the quartet–doublet mixing by anisotropic zfs interaction is important around the level-crossing regions ($r = r_1, r_2$ in Figure 1) for the generation of net CIDEP.^{16–21} Shushin^{14,19,20} formulated the magnitude of net polarization on free radical in both RTPM mechanisms. Adrian²¹ also presented the formula of the net polarization in the large exchange interaction limit. However, there were few experimental data to explain the mechanism of net CIDEP generation except for the study reported by Goudsmit et al.¹⁴ and Obi and his co-workers.^{11,12,16,17}

Thus far, quenching processes of excited molecules by free radicals have been mainly investigated by optical measurements. For example, the mechanism of quenching of the excited triplet states by radicals has been mainly discussed on the basis of deactivation rates of T–T absorption in the presence of free radicals.^{1–4} The transient absorption studies do not give direct information about the interaction between an excited molecule and a free radical. Hence, discussions about the intermolecular interaction were relatively obscure. On the other hand, by time-resolved ESR (TR-ESR) technique, one can directly observe the free radicals that experienced an intermolecular interaction between a radical and an excited molecule through CIDEP signals. Especially, CIDEP intensity contains information on the dynamics in the initial photochemical and photophysical processes. Thus, it is expected that we can quantitatively obtain information about the photophysical intermolecular interaction between an excited triplet molecule and a free radical.

Particularly, electron exchange interaction between the transient paramagnetic species is one of the important intermolecular interactions for the photoreaction dynamics. The exchange interaction in radical pairs has been widely studied by TR-ESR spectroscopy,^{25,26,35–39} and information about the exchange interaction has been obtained from the electron spin polarization generated by the RPM^{25,26,35–37,39} and from TR-ESR spectra of spin-correlated radical pairs (SCRPs).^{37,38} Quite recently, a TR-ESR spectrum of biradicals was analyzed based on a relaxation mechanism including the J modulation caused by conformational motion in a radical pair.³⁸ Contrary to the

radical pair system, there is little information about the electron exchange interaction in the system of the radical and excited triplet molecule, which is an important interaction for the photochemical dynamics in the more complex paramagnetic systems.

In this paper, we measured absolute magnitudes of electron spin polarization generated through the quenching of the excited triplet states of 1-chloronaphthalene (1CN), benzophenone (BP), and benzil by TEMPO radical in benzene by TR-ESR spectroscopy. In the 1CN–TEMPO system, viscosity dependence on the net polarization was observed in the temperature region 226–275 K in 2-propanol. From the theoretical and quantitative analysis, it is confirmed that the net electron spin polarization in RTPM is predominantly generated in the level-crossing regions. We propose a theoretical treatment to calculate the magnitudes of net polarization generated by the level crossings in the radical–triplet pair mechanism under viscous conditions and performed a numerical analysis of the net RTPM polarization with the stochastic-Liouville equation. From the analysis, it will clearly be demonstrated that efficiency of the CIDEP generation caused by RTPM is quite high under viscous conditions, and the magnitude of exchange interaction in a radical–triplet pair will be estimated. The quenching mechanism will also be discussed by comparing the works using optical measurements with those using TR-ESR spectroscopy.

2. Experimental Section

A conventional X-band ESR spectrometer (Varian E-112) was used to measure TR-ESR spectra. Transient ESR signals obtained without field modulation were transferred to a boxcar integrator (Stanford SR-250) for spectrum measurements or a digital oscilloscope (Techtronix TDS 350) for CIDEP decay profiles. The data in these instruments were transferred to personal computers. The time resolution of our system was about 200 ns. The gate time of the boxcar integrator was opened for 0.5 μ s. Microwave power was fixed at 5 mW. The excitation light source was a XeCl excimer laser (Lambda Physics LPX 100). Details of the equipment and method were described previously.²² Benzophenone and benzil (Tokyo Kasei) were recrystallized from GR grade *n*-hexane and ethanol, respectively. GR grade C₆₀ (Buckey), 1-chloronaphthalene (Tokyo Kasei), and TEMPO (Aldrich) were used as received. GR grade benzene, 2-propanol, and ethylene glycol (Tokyo Kasei) were used as solvents without further purification. The solution was degassed by bubbling Ar gas and was flowed through a quartz flat cell in an ESR cavity. The temperature was controlled by flowing cold nitrogen gas with an MTC-200HL (Micro Device) variable-temperature cryosystem. The temperature of the sample solution in the ESR cavity was measured with a thermometer. Optical densities of sample solutions at 308 nm were determined by a UV–vis spectrometer (Shimadzu). In laser flash photolysis experiments, a xenon flash lamp (Ushio XUL150DS) was used as a monitoring light source. The monitoring light passing through a monochromator (Nikon P250) was detected with a photomultiplier tube (Hamamatsu Photonics R928).

3. Results

Magnitudes of RTPM Polarization. Figure 2 shows the TR-ESR spectra obtained by 308 nm laser excitation in the systems of (a) 1CN–TEMPO and (b) C₆₀–TEMPO in benzene solution under the same experimental conditions at room temperature. In both TR-ESR spectra, three peaks appeared at the same positions as the peaks of TEMPO in the steady-state

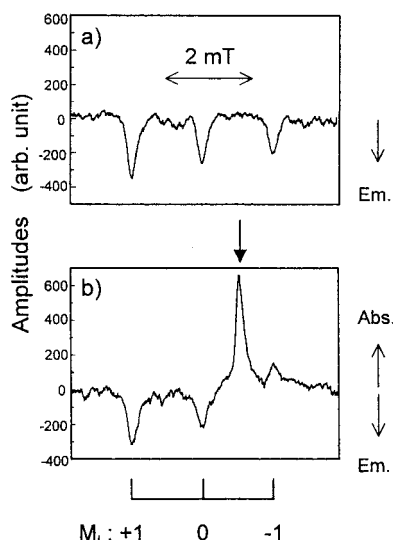
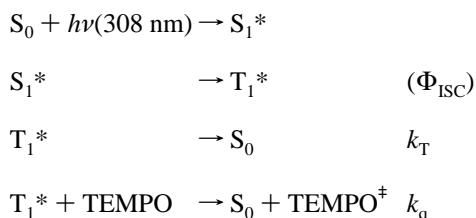


Figure 2. Time-resolved ESR spectra in (a) 1-chloronaphthalene— and (b) C_{60} —TEMPO systems observed at 1.2 μ s after the 308 nm laser excitation in benzene at room temperature. Optical densities at 308 nm of sample solution are a) 0.31 and (b) 0.22. In both measurements, concentrations of TEMPO are 1.95 mM.

ESR spectrum. Hence, signals of these three peaks were assigned to spin-polarized TEMPO radicals. This polarization is caused by quenching of the excited triplet molecules with radicals, as is interpreted in terms of RTPM reported in the previous studies in the same excited molecule—radical systems.^{12,15} One strong absorptive peak marked by an arrow in Figure 2b was assigned after Goudsmit and Paul¹⁵ to the lowest excited triplet state of C_{60} , which was not quenched by TEMPO radical in this time window.

In the C_{60} —TEMPO system, relative peak intensity of TEMPO is almost the same with the CIDEP spectrum obtained by Goudsmit and Paul¹⁵ in toluene. CIDEP patterns of TEMPO shown in Figure 2 are different from each other; in the C_{60} —TEMPO system, hyperfine-dependent E^*/A polarization is dominant, while in the 1CN—TEMPO system, net emissive polarization is dominant. As for the net CIDEP in RTPM, the polarization is generated by the state mixing between quartet and doublet states in radical—triplet pairs where the exchange interaction is effective (see Figure 1), and the state mixing is induced by zero-field splitting interaction of the counter triplet molecule.^{10–17} Because the D value of $^3C_{60}$ is much smaller (0.01 cm^{-1})^{30–32} than that of ^31CN (0.1 cm^{-1}),²⁴ net emissive polarization is weak in the C_{60} —TEMPO system, but strong in the 1CN—TEMPO system.

To discuss quantitatively the magnitude of CIDEP of TEMPO, we examine what factors control the signal intensities. RTPM polarization is generated on TEMPO through quenching of T_1 molecules (T_1^*) by radicals in the following scheme.



where Φ_{ISC} represents the quantum yield of intersystem crossing from the S_1 to T_1 state, and k_T and k_q are the rate constants of unimolecular deactivation of the triplet state and quenching of the T_1 molecule by TEMPO, respectively. TEMPO^\ddagger represents

the free radical that experienced the quenching of the T_1 molecule and possesses a certain amount of spin polarization caused by RTPM. In this scheme, the initial concentration of excited triplet was estimated to be about 2×10^{-5} M from the laser power, the optical density of the sample solution, and the volume of the irradiated part of the cell. Even if the triplet—triplet annihilation rate constants in both molecules are diffusion limited, this process is neglected under our experimental condition because of too low a concentration of excited triplet molecules. By this scheme, as described by Blättler and Paul²⁸ based on Bloch equations proposed by Verma and Fessenden,⁴⁰ the magnetization on TEMPO radicals is written as follows:

$$\frac{dM_y}{dt} = -\frac{M_y}{T_2} + \omega_1 M_z \quad (1)$$

$$\frac{dM_z}{dt} = -\omega_1 M_y + \frac{P_{\text{eq}}[\text{TEMPO}] - M_z}{T_1} + P_{\text{RTPM}} k_q [\text{TEMPO}][T_1^*] \quad (2)$$

$$\frac{d[T_1^*]}{dt} = -k_q [\text{TEMPO}][T_1^*] - k_T [T_1^*] \quad (3)$$

where M_i represents the magnetization in its direction in the rotating frame, ω_1 is the microwave field strength, and T_1 and T_2 are the spin—lattice and spin—spin relaxation times, respectively. P_{eq} and P_{RTPM} denote the magnitude of thermal equilibrium and RTPM spin polarization generated on the TEMPO radical. In the equations, M_y corresponds to the CIDEP signal intensity (I_{RTPM}). In our TR-ESR measurements, Boltzmann polarization of TEMPO can be hardly detected since the signals corresponding to the steady-state polarization of P_{eq} are eliminated by a preamplifier, as reported by Turro et al.³³ Thus, we regard $P_{\text{eq}} \ll P_{\text{RTPM}}$ in eq 2.

Under the experimental condition that T_1 , T_2 , and ω_1 are constant in both excited molecule—TEMPO systems as in Figure 2, I_{RTPM} at t_{obs} (1.2 μ s in the present experiment) after the laser excitation is written in the simple form as follows:¹⁷

$$I_{\text{RTPM}} = c P_{\text{RTPM}} I_L (1 - 10^{-\text{OD}}) \Phi_{\text{ISC}} \Phi_q \times [1 - \exp\{-(k_T + k_q [\text{TEMPO}])t_{\text{obs}}\}] \quad (4)$$

$$\Phi_q = \frac{k_q [\text{TEMPO}]}{k_T + k_q [\text{TEMPO}]} \quad (5)$$

where c is a constant depending on spin relaxation times and experimental conditions. I_L and OD represent laser power and optical density of the sample solution, respectively. From eq 4, a P_{RTPM} value in the 1CN—TEMPO system relative to P_{RTPM} in the C_{60} —TEMPO system is obtained from CIDEP signal intensities in Figure 2 measured under the same experimental conditions, i.e., the same gate time window and microwave power. The relative P_{RTPM} value (P_{RTPM}^x) to P_{RTPM} in the C_{60} —TEMPO system (P_{RTPM}^r) is expressed from eq 4 as follows:

$$\frac{P_{\text{RTPM}}^x}{P_{\text{RTPM}}^r} = \frac{I_{\text{RTPM}}^x}{I_{\text{RTPM}}^r} \times \frac{\Phi_{\text{ISC}}^r \Phi_q^r (1 - 10^{-\text{OD}(r)}) [1 - \exp\{-(k_T^r + k_q^r [\text{TEMPO}])t_{\text{obs}}\}]}{\Phi_{\text{ISC}}^x \Phi_q^x (1 - 10^{-\text{OD}(x)}) [1 - \exp\{-(k_T^x + k_q^x [\text{TEMPO}])t_{\text{obs}}\}]} \quad (6)$$

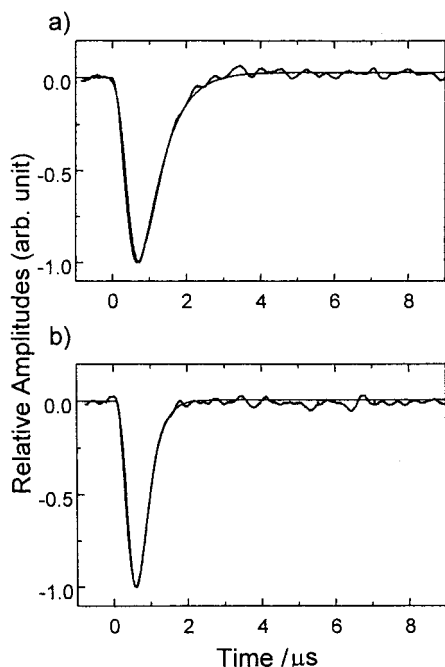


Figure 3. Time profiles of CIDEP signals of TEMPO in benzene observed and simulated at the peak $M_I = 0$ in (a) 1-chloronaphthalene– and (b) C_{60} –TEMPO systems at room temperature. In both measurements, the concentration of TEMPO is 1.95 mM.

where superscripts x and r denote the desired molecule–TEMPO and C_{60} –TEMPO systems, respectively. In Figure 2, optical densities of 1CN and C_{60} at 308 nm in the 0.5 mm interior cell were 0.31 and 0.22, respectively. Φ_{ISC} of 1CN²⁴ and C_{60} are reported²⁹ to be 0.79 and 1.0. The concentration of TEMPO was fixed at 1.95 mM, and other experimental conditions (laser power, signal sensitivity, gate time, and microwave power) were the same in both systems. Since $k_q[\text{TEMPO}] (> \sim 2 \times 10^6 \text{ s}^{-1})$ is much larger than k_T values (triplet lifetimes of C_{60} ¹⁵ and 1CN²⁴ are 8 and 280 μs , respectively) under our experimental conditions, k_T in eq 6 can be neglected. To determine the triplet quenching rate, time profiles of CIDEP signals of peaks at $M_I = 0$ of TEMPO were measured in both systems at the same radical concentration of 1.95 mM as shown in Figure 3. The profiles were simulated by using eqs 1–3 for the kinetics of the RTPM polarization: generation of the spin polarization by quenching of triplet molecules and spin relaxation in the TEMPO radical. Parameters used in the equations were as follows. Under our experimental condition of 5 mW microwave power, ω_1 is known to be $9.5 \times 10^5 \text{ rad s}^{-1}$ in our ESR cavity. T_2 of TEMPO is the reported value in toluene (65 ns) in both systems.¹⁵ In eq 3, the rise of triplet states is not considered due to very fast S_1 – T_1 intersystem crossing rates of 1CN ($4.2 \times 10^8 \text{ s}^{-1}$)²⁴ and C_{60} . Then, the time development of M_y , which was numerically solved with eqs 1–3, was convoluted with the response function of the spectrometer, and the best fitted profiles are shown in Figure 3 by using T_1 and k_q as parameters. In both systems, the T_1 value was determined to be 270 ns, which was almost the same as T_1 determined with the similar procedure in the C_{60} –TEMPO system in toluene at room temperature.¹⁵ Triplet quenching rates were determined to be $k_q[\text{TEMPO}] = 1.8 \times 10^6$ and $6.0 \times 10^6 \text{ s}^{-1}$ in the 1CN–TEMPO and C_{60} –TEMPO systems, respectively. The simulated profiles superimposed in Figure 3 agree well with the experimental results. It is noted that, under the experimental condition of ~ 2 mM TEMPO, the signal rises and decays in RTPM CIDEP are

governed by the spin–lattice relaxation of TEMPO and triplet quenching rates, respectively, as seen from Figure 3.

From eq 6, RTPM polarization ($P_{\text{RTPM}}^{1\text{CN}}/P_{\text{RTPM}}^{C_{60}}$) of TEMPO in the 1CN–TEMPO system relative to that in the C_{60} –TEMPO system was determined by using the signal intensities obtained and the parameters described above. The magnitude of spin polarization in the C_{60} –TEMPO system was reported in toluene,¹⁵ but the CIDEP spectrum in Figure 2b was measured in benzene. In both solvents, CIDEP patterns of TEMPO observed are almost the same, and hyperfine-dependent E^*/A polarization is dominant.¹⁵ Since the ratio of the viscosity²⁴ of benzene to toluene is only 1.1, TEMPO will have almost the same magnitude of polarization in benzene and toluene solutions;^{11,25} magnitudes of spin polarization of TEMPO in Figure 2b are -2.7 , -1.7 , and $1.3 P_{\text{eq}}$ at the peaks of $M_I = +1$, 0, and -1 , respectively, where P_{eq} represents the thermal equilibrium electron spin polarization.¹⁵ Magnitudes of spin polarization ($P_{\text{RTPM}}^{1\text{CN}}$) in the 1CN–TEMPO system were determined to be -3.1 , -2.4 , and $-1.9 P_{\text{eq}}$ at $M_I = +1$, 0, and -1 peaks, respectively, in benzene at room temperature.

Although net emissive polarization is dominant at the peak of $M_I = 0$, this peak still contains a little emissive polarization from the multiplet E^*/A pattern. The contribution of the multiplet effect at $M_I = 0$ was determined from the signal intensities in observed TR-ESR spectra and simulated relative intensities of the multiplet E^*/A spectrum of TEMPO. The spectrum due to the multiplet effect was simulated with RTPM theory reported in the previous study,¹¹ assuming that the g value of triplet 1CN was 2.003. The minor multiplet contribution was subtracted from P_{RTPM} at $M_I = 0$ to obtain the polarization factor of net RTPM (P_n). In the 1CN–TEMPO system, P_n was determined to be $-2.2 P_{\text{eq}}$. By the same procedure, P_{RTPM} in other excited molecule–TEMPO systems were estimated in benzene from eq 6, i.e., from I_{RTPM} measured under the same experimental conditions as in the C_{60} –TEMPO system; the P_{RTPM} value at each hyperfine state was determined using the values of OD, Φ_{ISC} ,²⁴ and $k_q[\text{TEMPO}]$ in each system.¹⁷ P_n values were determined in the systems of benzil (BZ)– and benzophenone (BP)–TEMPO to be -8.0 and $-6.9 P_{\text{eq}}$,¹⁷ respectively, in benzene at room temperature. Absolute magnitudes of net RTPM polarization obtained in the present experiments are listed in Table 1.

Temperature Effect on Net RTPM Polarization. Figure 4 shows the temperature effect on steady-state and TR-ESR spectra of TEMPO obtained in the 1CN–TEMPO system in 2-propanol. All experimental conditions except for temperature were the same in these measurements. In the steady-state ESR spectra (a and c in Figure 4), the peak intensity at $M_I = 0$ becomes slightly strong with decreasing temperature, although their line widths are almost the same. This is mainly due to the increase in the solute concentration caused by a slight increase in solvent density, as discussed later. As discussed above, peak intensities at $M_I = 0$ of TR-ESR spectra in Figure 4 mostly originate from the spin polarization due to net effect. It is noticeable that the CIDEP intensity depends strongly on temperature; CIDEP intensity becomes drastically strong with decreasing temperature, or net emissive polarization gets strong. Under our experimental conditions, the relative diffusion coefficient (D_r) in the 1CN–TEMPO system in 2-propanol was estimated to decrease from $\sim 6 \times 10^{-6}$ to $\sim 2 \times 10^{-6} \text{ cm}^2 \text{ s}^{-1}$ with reducing the temperature from 275 to 251 K. Details for determination of the D_r values are discussed later. Goudsmit et al.¹⁴ investigated temperature dependence of CIDEP generated through interaction between excited triplet benzophenone and

TABLE 1: Absolute Magnitudes of Net Spin Polarization (P_n) in TEMPO Observed (obs) and Calculated (calc) in Excited Triplet Molecule–TEMPO Systems in Benzene at Room Temperature (in Units of Boltzmann Polarization)

triplet species	D/cm^{-1}	P_n/P_{eq} (obs)	P_n/P_{eq} (calc)			
			ref 14 ^a	eq 20 ^b	eq 21 ^b	eq 22 ^c
1-chloronaphthalene	0.11	-2.2 ± 0.4	-0.4	-2.1	-2.5	-6.5
benzophenone	0.18	-6.9 ± 0.9	-1	-5.7	-6.7	-17
benzil	0.12	-8.0 ± 0.3	-0.4	-2.5	-3.0	-7.8
C_{60}	0.01	~ 0	0.0	0.0	0.0	-0.1

^a Calculated with the relaxation mechanism assuming exchange interaction at contact to be smaller than Zeemann energy. ^b Calculated with $3J_{\text{e}^{\text{ad}}} = -5.1 \times 10^{15} \text{ rad s}^{-1}$, $\lambda = 1.4 \text{ \AA}^{-1}$, $D_r = 5.0 \times 10^{-5} \text{ cm}^2 \text{ s}^{-1}$, and $\tau_c = 10 \text{ ps}$. ^c Calculated with $\tau_c > 40 \text{ ps}$ in eqs 20 and 21. See text for discussion.

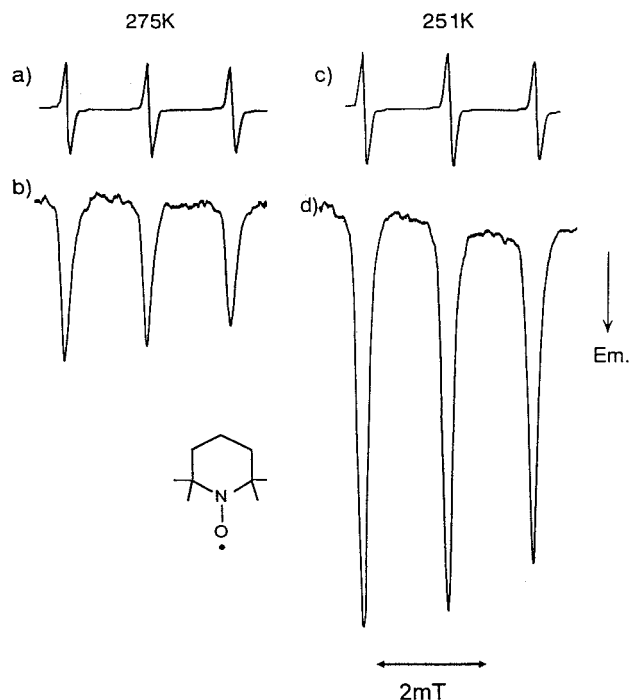


Figure 4. Temperature effect on the (a, c) steady-state and (b, d) time-resolved ESR spectra ($1.7 \mu\text{s}$ after the laser excitation) of TEMPO observed in the 1-chloronaphthalene (10 mM)–TEMPO (1.1 mM) system in 2-propanol.

TEMPO radical in 1,2-epoxypropane solution. In their study, the magnitude of net emissive polarization increased with decreasing temperature in the region of the D_r value larger than $\sim 1 \times 10^{-5} \text{ cm}^2 \text{ s}^{-1}$, but the net polarization did not increase in the region of smaller D_r than this value.¹⁴ On the other hand, in the triplet ICN–TEMPO system in 2-propanol, our experimental results indicate that the magnitude of net polarization increases drastically even when the D_r value decreases to much less than $10^{-5} \text{ cm}^2 \text{ s}^{-1}$.

To obtain temperature effects on the net RTPM polarization more quantitatively, time profiles of CIDEP at the $M_I = 0$ peak were measured at the temperature of 226–270 K. In the steady-state ESR spectra (a and c in Figure 4), the widths at $M_I = 0$ were almost the same (0.15 mT at 240–270 K). Since the signal sensitivity should be independent of temperature, as reported by Goudsmit et al.,¹⁴ the increase in steady-state ESR intensity at $M_I = 0$ in Figure 4 with decreasing temperature is caused by the increase in the (1) solvent density and (2) thermal equilibrium polarization, which obeys Curie relation ($P_{\text{eq}} = g\beta I(I + 1)B_0/3kT$, where I , B_0 , and k represent the electron spin quantum number, magnetic field, and Boltzmann constant, respectively). Therefore, the measured time profiles were calibrated with the steady-state ESR intensities at $M_I = 0$ obtained, and thermal equilibrium polarization was calculated with the Curie relation. The calibrated time developments of the relative magnetization

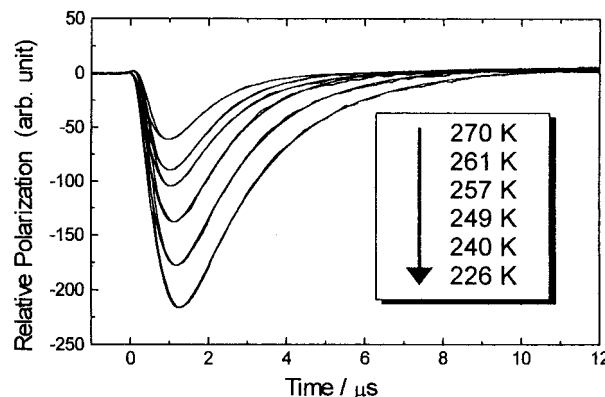


Figure 5. Temperature effect on time profiles of CIDEP signals at the peak $M_I = 0$ in TEMPO observed and simulated in the 1-chloronaphthalene (10 mM)–TEMPO (2 mM) system in 2-propanol.

TABLE 2: Viscosity Dependence on the Quenching Rate ($k_q[\text{TEMPO}]$) of Excited Triplet 1-Chloronaphthalene, Spin–Lattice Relaxation (T_1), and Net RTPM Polarization (P_n) of TEMPO in 2-Propanol

T/K	$D_r^a/10^{-6} \text{ cm}^2 \text{ s}^{-1}$	$k_q[\text{TEMPO}]^b/10^5 \text{ s}^{-1}$	T_1/ns	P_n (arb unit) ^c
270	4.8	8.8	340	-1.0
261	3.4	7.7	360	-1.5
257	2.8	7.0	360	-1.8
249	2.0	6.4	410	-2.2
240	1.3	5.3	420	-3.0
226	0.65	4.5	460	-3.8

^a Obtained from eq 7. ^b $[\text{TEMPO}] = 2 \text{ mM}$. ^c In units of P_n obtained at 270 K.

of TEMPO radicals are shown in Figure 5, together with the simulated ones. It is obvious that the net RTPM polarization drastically increases with decrease in temperature. The simulation of the profiles was done with Bloch equations (eqs 1–3) to obtain the magnitudes of RTPM polarization. Since the thermal equilibrium polarization of TEMPO cannot be detected with our TR-ESR measurements as described in the previous section, we discuss the relative magnitudes of P_{RTPM} compared to P_{RTPM} at 270 K. Parameters used in the equations were as follows. As described above, ω_1 is known to be $9.5 \times 10^5 \text{ rad s}^{-1}$ in our ESR cavity, and rapid S_1 – T_1 intersystem crossing and slow unimolecular decay of triplet ICN are negligible. T_2 was obtained to be 82 ns from the line widths of the steady-state ESR spectra shown in Figure 4. Signal rises and decays of RTPM CIDEP are attributed to T_1 and $k_q[\text{TEMPO}]$, respectively, as mentioned above. Thus, relative P_{RTPM} values can be obtained by fitting $M_y(t)$ calculated from Bloch equations to the relative signal intensities in the profiles as shown in Figure 5. The parameters determined are listed in Table 2 together with the diffusion coefficients (D_r) for the relative motion of the radical and triplet molecule in 2-propanol, which were estimated from the reported value of diffusion coefficient of benzophenone (D_{BP}) in 2-propanol at room temperature mea-

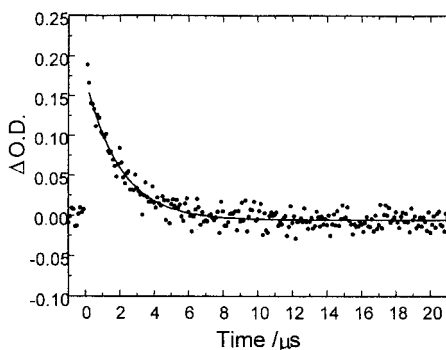


Figure 6. Transient absorption decay profile of excited triplet 1-chloronaphthalene monitored at 420 nm in the presence of 2.0 mM TEMPO in ethylene glycol at 20 °C. Lifetime of the triplet state was determined to be 2.0 μ s.

sured with the transient grating method by Terazima et al.²³ They reported that the diffusion coefficient of benzophenone (D_{BP}) in 2-propanol at room temperature was $6.8 \times 10^{-6} \text{ cm}^2 \text{ s}^{-1}$ and that the D_r value was inversely proportional to the solvent viscosity. In this study, the molecular radii of the triplet 1CN and TEMPO were assumed to be the same as that of benzophenone ($a = 3.7 \text{ \AA}$). Therefore, from the Stokes–Einstein relationship, D_r values were determined with D_{BP} , viscosity (η), and temperature (T) as

$$D_r = 2D_{BP} \frac{\eta_{298K} T}{\eta_T 298} \quad (7)$$

where the viscosity of 2-propanol was reported³⁵ to obey $\eta_T = 4.47 \times 10^{-4} \exp(2532/T) \text{ cP}$. The D_r values estimated from eq 7 may have errors caused by the differences in molecular size, which would however be within a factor of 20%.

To check the accuracy of viscosity in our TR-ESR experiments at low temperature, the T–T absorption decay profile of excited triplet 1CN was measured in the presence of 2.0 mM TEMPO in ethylene glycol ($\eta = 20 \text{ cP}$) at 20 °C with the laser flash photolysis technique as shown in Figure 6. According to eq 7, D_r in ethylene glycol is estimated to be $1.3 \times 10^{-6} \text{ cm}^2 \text{ s}^{-1}$ at 293 K, which is almost the same as D_r at 240 K in 2-propanol. (See Table 2.) The quenching rate constant was obtained to be $k_q = 2.5 \times 10^8 \text{ M}^{-1} \text{ s}^{-1}$ from the decay profile in Figure 6, which was almost the diffusion limit in ethylene glycol and was quite close to the rate obtained from the time profiles in Figure 5 at 240 K ($k_q = 2.7 \times 10^8 \text{ M}^{-1} \text{ s}^{-1}$) in 2-propanol. Therefore, D_r values estimated from eq 7 in 2-propanol will be valid even in the lower temperature region in Table 2.

As described above, contributions of the multiplet effect at $M_I = 0$ were subtracted from P_{RTPM} to obtain the polarization factor of net RTPM (P_n in Table 2). In Figure 7, the relative magnitudes of net RTPM polarization of P_n were plotted against the values of $1/D_r$. It is evident that P_n is almost proportional to $1/D_r$ (or viscosity) in the region of $D_r = 2 \times 10^{-6}$ to $5 \times 10^{-6} \text{ cm}^2 \text{ s}^{-1}$. It is noticeable that the feature of viscosity dependence on the net polarization is quite different from the result reported in the benzophenone–TEMPO system in 1,2-epoxypropane.¹⁴

4. Theory

To interpret the experimental results, it is important to analyze theoretically the spin dynamics in the radical–triplet pair system. Two types of CIDEP mechanisms have been considered for the generation of the net RTPM polarization resulting from the state

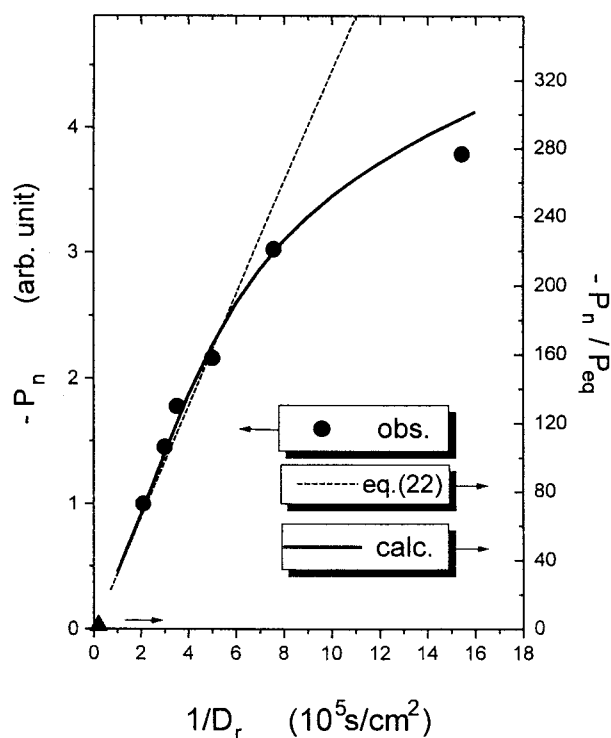


Figure 7. Plots of viscosity dependence on the magnitudes of net RTPM polarization (●) obtained with the present experiment in arbitrary units, (⋯) calculated with the analytical form of eq 22, and (—) calculated with the numerical analysis of SLE in eq 13 in the 1-chloronaphthalene–TEMPO system. Both calculated results are in units of thermal equilibrium polarization (P_{eq}) at room temperature. (▲) $P_n = -2.2 P_{eq}$ experimentally obtained in benzene (at $D_r = 5.0 \times 10^{-5} \text{ cm}^2 \text{ s}^{-1}$).

mixing between the quartet and doublet states in the pair. The mechanisms are mainly classified with the magnitude of exchange interaction, that is, the energy splitting ($-3J_0$) between the quartet and doublet states at the closest approach in the radical–triplet pair (see Figure 1).^{19,20} When $-3J_0$ is smaller than the Zeeman energy, the radical and triplet molecule cannot approach closer to the level-crossing regions ($r = r_1$ and r_2 in Figure 1) than the encounter point. Therefore, the state mixing will occur in the region of $r > r_2$. On the other hand, when $-3J_0$ is much larger than the Zeeman energy, the quartet–doublet mixing through anisotropic zfs interaction will be dominant in the level-crossing regions. In the former case, Shushin^{19,20} and Goudsmit et al.¹⁴ proposed a theoretical analysis of the magnitude of spin polarization in detail. In this section, we discuss the theory of spin dynamics in the case of large exchange interaction reported previously^{16–21} for deriving an analytical form^{17–21} and perform numerical calculations of the magnitude of net RTPM polarization.

Spin dynamics in a radical–triplet pair system is described by the stochastic-Liouville equation (SLE), in which effects of spin interactions and relative molecular diffusion are considered as

$$\frac{\partial r \hat{\rho}(r,t)}{\partial t} = -i[\hat{H}(r), r\hat{\rho}(r,t)] + D_r \frac{\partial^2 r \hat{\rho}(r,t)}{\partial r^2} \quad (8)$$

where $\rho(r,t)$ is the density matrix of the radical–triplet pair at time t and pair separation r . The spin Hamiltonian $\hat{H}(r)$ is represented as follows:¹⁶

$$\hat{H}(r) = \beta(g_T \hat{S}_T + g_R \hat{S}_R) B_0 + D \left(\hat{S}_{T\zeta}^2 - \frac{1}{3} \hat{S}_T^2 \right) - 2J(r) \hat{S}_T \hat{S}_R \quad (9)$$

$$\frac{\partial r \rho_0}{\partial t} = D_r \frac{\partial^2 r \rho_0}{\partial r^2} \quad (13a)$$

where the symbols have their usual meanings. Subscripts T and R represent the triplet molecule and radical, respectively. D represents the D value of zfs interaction of triplet molecule. In eq 9, the E value (typically $< 0.01 \text{ cm}^{-1}$) is neglected due to its small contribution compared to the D value ($\sim 0.1 \text{ cm}^{-1}$ in 1CN). ζ indicates an eigenaxis of zfs interaction in the frame of the triplet molecule. $J(r)$ is the exchange interaction in the pair and is assumed to be dependent only on r . We employ a usual form of an exponentially decaying exchange interaction,

$$J(r) = J_0 \exp\{-\lambda(r-d)\} \quad (10)$$

where d is the distance of closest approach in the pair. In the presence of electron exchange interaction between the radical and triplet molecule, spin wave functions of the pair are written as the eigenstates of the exchange interaction as follows:

$$|Q_{3/2}\rangle = |\alpha_1 \alpha_2 \alpha_R\rangle \quad (11a)$$

$$|Q_{1/2}\rangle = \frac{1}{\sqrt{3}} (|\alpha_1 \alpha_2 \beta_R\rangle + |\alpha_1 \beta_2 \alpha_R\rangle + |\beta_1 \alpha_2 \alpha_R\rangle) \quad (11b)$$

$$|Q_{-1/2}\rangle = \frac{1}{\sqrt{3}} (|\beta_1 \beta_2 \alpha_R\rangle + |\beta_1 \alpha_2 \beta_R\rangle + |\alpha_1 \beta_2 \beta_R\rangle) \quad (11c)$$

$$|Q_{-3/2}\rangle = |\beta_1 \beta_2 \beta_R\rangle \quad (11d)$$

$$|D_{1/2}\rangle = \frac{1}{\sqrt{6}} (2|\alpha_1 \alpha_2 \beta_R\rangle - |\alpha_1 \beta_2 \alpha_R\rangle - |\beta_1 \alpha_2 \alpha_R\rangle) \quad (11e)$$

$$|D_{-1/2}\rangle = \frac{1}{\sqrt{6}} (2|\beta_1 \beta_2 \alpha_R\rangle - |\beta_1 \alpha_2 \beta_R\rangle - |\alpha_1 \beta_2 \beta_R\rangle) \quad (11f)$$

where subscripts in the spin function of α or β denote triplet molecule (1 and 2) and radical (R). As described above, we assume that $-J_0$ is much larger than the Zeeman splitting ($-J_0 \gg g\beta B_0$) and discuss the state mixing between $|Q\rangle$ and $|D\rangle$ through $\hat{H}(r)$ around the level-crossing regions ($r = r_1$ and r_2). As an example, the mixing between $|Q_{-3/2}\rangle$ and $|D_{-1/2}\rangle$ around $r = r_2$ is discussed below. The matrix elements of $\hat{H}(r)$ for the quartet–doublet mixing are expressed from eqs 9 and 11, assuming $g_R = g_T = g$, as follows:

$$\hat{H}(r) = \begin{bmatrix} |Q_{-3/2}\rangle & |D_{-1/2}\rangle \\ -\frac{3}{2}g\beta B_0 + \frac{3 \cos^2 \theta - 1}{6}D - J(r) & \frac{\sin \theta \cos \theta}{\sqrt{6}} \exp\left\{i\left(\frac{\pi}{2} - \varphi\right)\right\} D \\ \frac{\sin \theta \cos \theta}{\sqrt{6}} \exp\left\{i\left(\varphi - \frac{\pi}{2}\right)\right\} D & -\frac{1}{2}g\beta B_0 + 2J(r) \end{bmatrix} \quad (12)$$

where θ and φ represent the angles of the ζ axis along the laboratory coordinates visualized in our previous study.¹⁶ Because triplet molecules are randomly oriented along the magnetic field B_0 , the second term of $\langle Q_{-3/2} | \hat{H}(r) | Q_{-3/2} \rangle$ averages zero due to $\langle \cos^2 \theta \rangle = 1/3$. From eqs 8 and 12, the following relationships are obtained:

$$\frac{\partial r \rho_v}{\partial t} = D_r \frac{\partial^2 r \rho_v}{\partial r^2} + \mathbf{\Omega}(r) \times r \rho_v \quad (13b)$$

$$\mathbf{\Omega}(r) = \begin{pmatrix} \frac{2 \sin \theta \cos \theta}{\sqrt{6}} \sin \varphi D \\ \frac{2 \sin \theta \cos \theta}{\sqrt{6}} \cos \varphi D \\ \omega_0 + 3J(r) \end{pmatrix}, \quad \rho_v(r, t) = \begin{pmatrix} \rho_x \\ \rho_y \\ \rho_z \end{pmatrix} \quad (14)$$

Here, ρ represents the matrix element of the density matrix, and $\rho_0 = C_D C_D^* + C_Q C_Q^*$, $\rho_x = C_Q C_D^* + C_D C_Q^*$, $\rho_y = -i(C_Q C_D^* - C_D C_Q^*)$, and $\rho_z = C_D C_D^* - C_Q C_Q^*$, where $C_Q(t)$ and $C_D(t)$ are the coefficients of the wave function, $\psi(t) = C_Q(t)|Q_{-3/2}\rangle + C_D(t)|D_{-1/2}\rangle$, in the SLE. ω_0 denotes Zeeman splitting between the quartet and doublet states, and in this case, $\omega_0 = g\beta B_0$. As visualized in our previous study,¹⁶ the mechanism of net RTPM generation is clearly understood by the vector model of eqs 13 and 14, which is quite similar to the model of $S-T_{\pm 1}$ mixing in RPM proposed by Adrian and Monchick.²⁶ The SLE in the other crossing region ($r = r_1$) was previously obtained with almost the same procedure discussed above.¹⁶ The transition probability caused by a level crossing is represented as the difference in the ρ_z component in the ρ_v vector as^{16,25,26}

$$\Delta \rho_z \equiv \lim \int_d^\infty (\rho_0 - \rho_z) r^2 dr \quad (15)$$

Here, we treat the case of the high field approximation ($B_0 \sim 3400 \text{ G}$), where the quartet–doublet state mixing is dominant around the level-crossing regions. In the system of Figure 1, total net polarization is represented as a sum of the polarization generated in the level-crossing regions and is obtained from eqs 11 and 15 as follows:^{17,25}

$$P_n = -2 \lim \int_d^\infty \text{tr}\{S_{Rz} r \rho(r, t)\} r dr \approx \frac{1}{3} \Delta \rho_z(r_1) + \frac{2}{3} \Delta \rho_z(r_2) \quad (16)$$

In our theoretical treatment of eqs 8, 9, and 12–14, the anisotropic zfs interaction (H_{zfs}) is assumed to be static or time-independent. In the limit of slow diffusion ($g\beta B_0 \tau_c \gg 1$, where τ_c is the rotational correlation time of the triplet molecule) and large exchange interaction ($-J_0 g\beta B_0$), the effect of fluctuating H_{zfs} is eliminated since orientation of a triplet molecule is preserved when passing through the level-crossing region. Therefore, eq 13 is applicable under viscous conditions. The total spin polarization is obtained as an average of CIDEP generated from all molecular orientations along the magnetic field. In the level-crossing region ($\omega_0 = -3J(r_2)$), the quartet–doublet mixing rate induced by H_{zfs} of a triplet molecule is represented from eq 14 as $|\mathbf{\Omega}| = 2 \cos \theta \sin \theta D/\sqrt{6} \text{ rad s}^{-1}$. To analyze approximately the magnitude of net RTPM polarization as an average for the angle of θ , $\langle \cos \theta \sin \theta \rangle = 1/3$ is put in eq 14 for the numerical analysis. By employing a finite-difference technique in r , time development of the density matrix can be numerically solved at each r value from eqs 13 and 14 under the initial condition that the doublet states in the radical–triplet pair are selectively quenched through the triplet quenching

process and the quartet states are initially populated at the closest pair separation,

$$\rho_v(d,0) = \begin{pmatrix} 0 \\ 0 \\ -1 \end{pmatrix} \quad (17)$$

Shushin and Adrian separately formulated the analytical solutions of the electron spin polarization of eq 15 generated in a two-level system in the case where the mixing interaction (zfs interaction) fluctuates in the level-crossing region ($r = R_c$) with the correlation time τ_c , which can also be applicable under nonviscous conditions ($g\beta B_0\tau_c < 1$).

Shushin's formula^{19,20} is

$$\Delta\rho_z = \frac{\pi}{2} \text{sign}(J_0) \frac{\langle \Omega_x^2 \rangle + \langle \Omega_y^2 \rangle}{\omega_0} \frac{R_c}{\lambda D_r} \frac{1}{1 + (\omega_0\tau_c)^{-2}} \quad (18)$$

and Adrian's formula²¹ is

$$\Delta\rho_z = \text{sign}(J_0) \frac{\langle \Omega_x^2 \rangle + \langle \Omega_y^2 \rangle}{\omega_0} \frac{R_c}{\lambda D_r} \arctan(\omega_0\tau_c) \quad (19)$$

where Ω_x and Ω_y are the ρ_x and ρ_y components of $\Omega(r)$, respectively. Both formulas are derived with the assumption that the triplet quenching occurs at the distance close to $r = R_c$ and that the quartet–doublet transitions are “one-sided”; back transitions from doublet to quartet states are neglected.^{19,21} By substituting eqs 18 and 19 into eq 16, total magnitudes of net RTPM polarization are obtained as

$$P_n = \frac{2\pi}{135} \text{sign}(J_0) \frac{D^2}{g\beta B_0\lambda D_r} \left\{ \frac{r_1}{4 + (g\beta B_0\tau_c)^{-2}} + \frac{r_2}{1 + (g\beta B_0\tau_c)^{-2}} \right\} \quad (20)$$

and

$$P_n = \frac{1}{135} \text{sign}(J_0) \frac{D^2}{g\beta B_0\lambda D_r} \{ r_1 \arctan(2g\beta B_0\tau_c) + 4r_2 \arctan(g\beta B_0\tau_c) \} \quad (21)$$

respectively. P_n values are theoretically estimated from eqs 20 and 21 and can be compared quantitatively with the P_n values obtained experimentally. In the limit of slow diffusion ($g\beta B_0\tau_c \gg 1$) as in 2-propanol solution at low temperature, both eqs 20 and 21 give the same formula of the net RTPM polarization as

$$P_n = \frac{\pi}{270} \text{sign}(J_0) \frac{D^2(r_1 + 4r_2)}{g\beta B_0\lambda D_r} \quad (22)$$

which is proportional to $1/D_r$.

5. Discussion

Absolute Magnitudes of Net RTPM in Benzene. It is interesting to compare quantitatively the absolute magnitudes of net polarization obtained experimentally in benzene with those predicted theoretically by the RTPM mechanism. Goudsmit et al.¹⁴ proposed a relaxation mechanism for the quartet–doublet mixing induced by zfs interaction. According to their study, net CIDEP is predominantly generated in the regions outside the level crossing ($r > r_1, r_2$) in Figure 1, and the absolute magnitude of net polarization P_n is theoretically formulated using the SLE, assuming that the exchange interaction in a

radical–triplet pair is smaller than the Zeeman energy. In benzene solution at room temperature, the diffusion coefficient for the relative motion of TEMPO and triplet molecule is estimated to be about $5 \times 10^{-5} \text{ cm}^2 \text{ s}^{-1}$ from eq 7. If the exchange interaction is assumed to be smaller than Zeeman splitting¹⁴ ($-J_0 = 5.0 \times 10^9 \text{ rad s}^{-1}$), their mechanism predicts the P_n value to be $-0.4, -0.4,$ and $-1 P_{\text{eq}}$ in the 1CN–, benzil–, and benzophenone–TEMPO systems, respectively, all of which are much smaller than our experimental results. (See Table 1.) Therefore, our experimental results cannot be explained by this mechanism.

P_n values are obtained from eqs 20 and 21 in the fast diffusion ($g\beta B_0\tau_c < 1$) and large exchange interaction ($-J_0 \gg g\beta B_0$) limits. The following parameters were used in eqs 20 and 21 to evaluate the P_n values. Zeeman splitting obtained from the microwave counter ($g\beta B_0 = 6.0 \times 10^{10} \text{ rad s}^{-1}$ under our experimental condition) and the reported D value ($D = 2.1 \times 10^{10}, 2.3 \times 10^{10},$ and $3.4 \times 10^{10} \text{ rad s}^{-1}$ for triplet 1CN, benzil, and benzophenone, respectively) were used. The diffusion coefficient D_r in benzene was determined¹⁷ from eq 7 with the reported value of the diffusion constant of BP in benzene ($D_{\text{BP}} = 2.5 \times 10^{-5} \text{ cm}^2 \text{ s}^{-1}$ at room temperature)²⁹ to be $5.0 \times 10^{-5} \text{ cm}^2 \text{ s}^{-1}$. Correlation time τ_c was assumed to be 10 ps.¹⁷ The parameters in exchange interaction in a radical–triplet pair were assumed to be the same order of magnitude as in the transient radical pairs, and we put $3J_0e^{\lambda d} = -5.1 \times 10^{15} \text{ rad s}^{-1}$, $\lambda = 1.4 \text{ \AA}^{-1}$, and $d = 7 \text{ \AA}$. Then, the separations between the radical and triplet molecule at the level crossing are estimated as $r_1 = 7.6 \text{ \AA}$ and $r_2 = 8.1 \text{ \AA}$, which indicates that the quartet–doublet mixing occurs at 0.6 and 1.1 \AA away from the closest approach in the pair. In all the excited molecule–TEMPO systems, $D_r, \tau_c, J_0, d,$ and λ were assumed to be the same. For example, the P_n values in the 1CN–, BZ–, and BP–TEMPO systems were calculated as $P_n = -2.1, -2.5,$ and $-5.7 P_{\text{eq}}$ from eq 22, respectively. Moreover, we calculated P_n with eq 22, assuming that the molecular rotational correlation time is slower than ~ 40 ps. P_n values obtained experimentally and theoretically are summarized in Table 1 together with the reported D values. In the 1CN and BP systems, experimentally measured magnitudes of the P_n values agree well quantitatively with the ones calculated from eqs 20 and 21 and are about 3 times smaller than that calculated from eq 22. This result strongly suggests that the net RTPM polarization is generated in the level-crossing regions and that the anisotropic zfs interactions fluctuate in the level-crossing regions due to the effective rotational motions in benzene and make the net RTPM polarization weak. On the contrary, in the BZ–TEMPO system, observed $|P_n| = 8.0 P_{\text{eq}}$ is about 3 times larger than the calculated values from eqs 20 and 21, but agrees well with the calculated P_n ($=7.8 P_{\text{eq}}$) by using eq 22. Although we used estimated $r_i, D_r, \tau_c,$ and λ values to calculate P_n values, it is difficult to consider that the errors in r_i and λ make the P_n value 3 times large. Moreover, D_r cannot become 3 times smaller in the BZ–TEMPO system than in the other systems even if BZ molecular size is bigger than 1CN and BP. Therefore, in the BZ system, τ_c in the excited triplet BZ will be slower than 40 ps (that is, $g\beta B_0\tau_c \gg 1$) due to the bigger molecular size of BZ than that of 1CN and BP, and hence the orientation of triplet molecules may be preserved when passing through the level-crossing region. It is noted that in Debye's model the rotational correlation time is sensitive to the molecular size or radii (a), since $\tau_c \propto a^3$. In the previous study,¹¹ RTPM polarization of the OTEMPO radical generated by quenching of the excited triplet acetone was observed in benzene. In the acetone–OTEMPO system, net RTPM polarization was very weak compared with the hyperfine-dependent

multiplet polarization in spite the relatively large D value in triplet acetone (0.15 cm^{-1}). This result is considered to be caused by the effective fluctuation of the zfs interaction in the level-crossing region due to the fast rotational correlation time of triplet acetone, contrary to the BZ system. If $\tau_c = 3 \text{ ps}$, $D_r = 5.0 \times 10^{-5} \text{ cm}^2 \text{ s}^{-1}$, and $D = 2.9 \times 10^{10} \text{ rad s}^{-1}$ are put in eq 20, the magnitude of net RTPM polarization is estimated to be $P_n = -0.6 P_{\text{eq}}$, which is 10 times smaller than the P_n value obtained in the BP-TEMPO system. At least in the molecular systems investigated here, it is concluded that the net RTPM polarization is generated in the two level-crossing regions and that the exchange interaction in the radical-triplet pair is stronger than the Zeeman energy.

For deeper understanding of the influence of the fluctuating zfs interaction of the triplet molecules, investigations on the microwave frequency dependence on the magnitude of net RTPM polarization will be very fruitful. For example, magnitudes of the net polarization in the 1CN-TEMPO system are predicted to be $-0.09 P_{\text{eq}}$ and $-4.7 P_{\text{eq}}$ from eq 20 in the L-band ($g\beta B_0 = 500 \text{ G}$) and Q-band ($g\beta B_0 = 10\,000 \text{ G}$) frequency regions, respectively. Thus, it may be difficult to detect the net RTPM CIDEP by the TR-ESR spectroscopy in lower than the X-band microwave frequency region, since the fluctuation of the zfs interactions in the level crossings is more effective due to $g\beta B_0 \tau_c \ll 1$.

Numerical Analysis of Viscosity Dependence on Net RTPM Polarization. As theoretically predicted by Shushin^{19,20} and Adrian,²¹ investigations of the viscosity ($1/D_r$) dependence on the net polarization is important to examine the spin dynamics in net RTPM. In the limit of slow diffusion ($g\beta B_0 \tau_c \gg 1$) as in 2-propanol solution and large exchange interaction ($-J_0 \gg g\beta B_0$), the net polarization is proportional to $1/D_r$, as seen in eq 22. On the contrary, in the case of small exchange interaction ($-J_0 < g\beta B_0$), the relaxation mechanism¹⁴ predicts that the polarization is constant in the region of diffusion coefficient smaller than $10^{-5} \text{ cm}^2 \text{ s}^{-1}$. Thus, our experimental results cannot be explained by the relaxation mechanism with $-J_0 < g\beta B_0$.

According to the finite difference technique for the numerical analysis, time development of the density matrix is expressed in the following forms from the SLE of eq 13 as

$$\rho_0(r, t + \Delta t) = \rho_0(r, t) + h\{\rho_0(r + \Delta r, t) - 2\rho_0(r, t) + \rho_0(r - \Delta r, t)\} \quad (23a)$$

$$\rho_v(r, t + \Delta t) = \rho_v(r, t) + h\{\rho_v(r + \Delta r, t) - 2\rho_v(r, t) + \rho_v(r - \Delta r, t)\} + \Omega(r) \times \rho_v(r, t) \Delta t \quad (23b)$$

$$h = D_r \frac{\Delta t}{\Delta r^2} \quad (24)$$

To calculate the SLE, we use the boundary conditions reported by Freed and Pedersen:²⁵ At the closest approach in a radical-triplet pair, the hard-core repulsive interaction for $r < d$ leads to the reflective inner boundary condition as

$$\rho(d, t + \Delta t) = \rho(d, t) + h\{2\rho(d + \Delta r, t) - 2\rho(d, t)\} \quad (25)$$

and, in the outer region ($r = r_N$), the equations are represented as the collecting-wall boundary condition,

$$\rho(r - \Delta r, t + \Delta t) = \rho(r_N - \Delta r, t) + h\{\rho(r_N, t) - 2\rho(r_N - \Delta r, t)\} \quad (26a)$$

$$\rho(r_N, t + \Delta t) = \rho(r_N, t) + 2h\rho(r_N - \Delta r, t) \quad (26b)$$

which means the pair is collected and cannot diffuse back to the interacting regions. The same parameters were used for the exchange interaction and zfs constant in the 1CN-TEMPO system as described in the previous section: $D = 2.1 \times 10^{10} \text{ rad s}^{-1}$, $3J_0 e^{\lambda d} = -5.1 \times 10^{15} \text{ rad s}^{-1}$, $\lambda = 1.4 \text{ \AA}^{-1}$, and $d = 7 \text{ \AA}$. From eqs 14–17 and 23–26, time development of the density matrix at each pair separation was numerically solved until the $\rho_0 - \rho_z$ value in the outer region ($r = r_N$) becomes constant, and we obtained $\Delta\rho_z$ from eq 15. We calculated the $\Delta\rho_z$ values generated in the two level-crossing regions ($r = r_1$ and r_2) and obtained P_n values from eq 16 as a function of the $1/D_r$ value as shown in Figure 7. The numerical calculations were performed under two conditions: $r_N = 12 \text{ \AA}$ with $\Delta r = 0.025 \text{ \AA}$, and $r_N = 18 \text{ \AA}$ with $\Delta r = 0.05 \text{ \AA}$. In the calculations, Δt values were chosen to satisfy $h = 1/6$ in eq 24, which sufficiently gives the most accurate solutions of the diffusion eq 13a. Calculated results under the two conditions gave almost the same P_n values; at most, the difference was only 10% at the largest D_r value of $1.0 \times 10^{-5} \text{ cm}^2 \text{ s}^{-1}$. Thus, the analysis of $r_N = 18 \text{ \AA}$ with $D_r = 0.05 \text{ \AA}$ will be sufficient to reproduce the spin interaction and diffusion motion of the pair. Since effective regions of the quartet-doublet mixing through zfs interaction are quite close to the closest distance of the pair, the possibility of diffusing back from the defined outer region to the effective interacting regions will be quite small in a viscous solvent.

In Figure 7, the magnitudes of net emissive polarization calculated with eq 22 and numerical analysis of eq 13 or eqs 23–26 are plotted against $1/D_r$ in the units of Boltzmann polarization ($P_{\text{eq}} = 7.5 \times 10^{-4}$) at room temperature. In the region of $1/D_r < 7 \times 10^5 \text{ s cm}^{-2}$, the magnitudes of net emissive polarization calculated by numerical analysis agree well quantitatively with the ones calculated with eq 22 and are almost proportional to $1/D_r$. This result indicates that the numerical analysis is well compatible with the analytic form of eq 22 in the region of $1/D_r < 7 \times 10^5 \text{ s cm}^{-2}$. In Figure 7, P_n values (plotted with ●) were experimentally measured as relative magnitudes of spin polarization and are not in the units of Boltzmann polarization. As seen in Figure 7, the experimentally obtained net RTPM polarization was almost in proportion to $1/D_r$ in the region of $2 \times 10^5 < 1/D_r < 7 \times 10^5 \text{ (s cm}^{-2})$. This relationship is consistent with the results of the numerical calculation and the analytical solution of the SLE as seen in Figure 7. Moreover, as described in the previous section, the magnitude of net RTPM polarization ($-2.2 P_{\text{eq}}$) in benzene (plotted with ▲ in Figure 7) was well fitted quantitatively to the ones calculated from eqs 20 and 21 in the 1CN-TEMPO system. Therefore, the experimental results strongly indicate that the net emissive polarization is generated predominantly in the level-crossing regions and that the magnitude of the polarization amounts to about -70 to $-200 P_{\text{eq}}$ in the region of $2 \times 10^5 < 1/D_r < 7 \times 10^5 \text{ (s cm}^{-2})$ in the 1CN-TEMPO system.

In the region of $1/D_r > 7 \times 10^5 \text{ s cm}^{-2}$, the numerically calculated curve is not coincident with the line solved analytically from eq 22, although both of the calculations were based on the SLE in eq 13. The experimentally obtained $1/D_r$ dependence on the net polarization is well fitted to our numerical analysis rather than eq 22. Especially, under the most viscous conditions of $1/D_r = 1.6 \times 10^6 \text{ s cm}^{-2}$, eqs 20 and 21 predict the P_n value to be $-520 P_{\text{eq}}$, while our calculated value is $-300 P_{\text{eq}}$. When the analytical form of eqs 20 and 21 was derived from the SLE, transitions from the quartet to doublet states ($Q \rightarrow D$ transition) through H_{zfs} were only considered and $Q \leftarrow D$

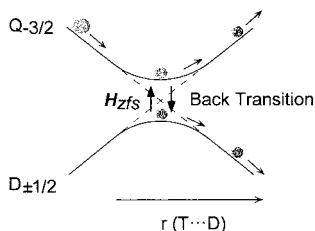


Figure 8. Schematic representation of population development of quartet and doublet states in radical–triplet pairs around the level-crossing region in the case of slow diffusion.

type back-transitions were neglected.^{19–21} This approximation is valid when the population of doublet state transferred from the quartet through H_{zfs} is small; that is eqs 20 and 21 can adequately predict the net RTPM polarization when its magnitude is small. On the other hand, under the more viscous conditions, the quartet–doublet mixing occurs more effectively in the level-crossing region. When the population of the doublet state transferred becomes comparable to the population of the quartet state, the $Q \leftarrow D$ type back-transition through H_{zfs} simultaneously occurs in the level-crossing region, as shown in Figure 8, and makes the P_n value smaller than those obtained from eqs 20 and 21. It is noted that, even if H_{zfs} accelerates the Q – D mixing much more effectively, the magnitude of net RTPM polarization cannot exceed the value of $1/2$ ($\Delta\rho_z < 1/2$), or the $|P_n|$ value must be smaller than $670 P_{eq}$. In our numerical analysis, we directly calculated the SLE in eq 13 and obtained the time development of the density matrix without the assumption that the quartet–doublet transition was “one-sided”, and hence the effect of the back-transition was reflected in our calculated results in Figure 7. This is confirmed with the result that the $|P_n|$ in the region of $1/D_r > 1.6 \times 10^6 \text{ s cm}^{-2}$ was calculated to be $>520 P_{eq}$ from eq 22, the magnitude of which is comparable to the polarization limit of $670 P_{eq}$. The good agreement between the experiment and the numerical analysis strongly indicates that the magnitude of net RTPM polarization is very large and amounts to $300 P_{eq}$ under the highly viscous conditions of $\eta > 20 \text{ cP}$ in the 1CN–TEMPO system.

The numerical calculations were performed with the parameter of $3J_0e^{\lambda d}$ to be -5.1×10^{15} and $-5.1 \times 10^{16} \text{ rad s}^{-1}$, as shown in Figure 9. The calculated viscosity dependencies on the net RTPM polarization were almost the same. This result is consistent with the approximated analytical form of eqs 20 and 21; Adrian²¹ suggested theoretically that the net emissive polarization is not directly dependent on the J_0 value. Although we could not determine the precise J_0 value by fitting the viscosity dependence on P_n in Figure 7, our experimental results strongly suggest that the net polarization is predominantly generated in the two level-crossing regions of radical–triplet pair and that in highly viscous solvent ($\eta > 20 \text{ cP}$) the magnitude of the polarization amounts to $300 P_{eq}$. The obtained large magnitudes of net RTPM polarization are not necessarily surprising results. Blättler et al.²⁸ investigated the net RTPM polarization generated through the quenching of the excited triplet benzil by benzyl radical at low temperature, and P_n was roughly estimated to be ca. $-50 P_{eq}$, which cannot be reproduced by the relaxation mechanism with $-J_0 < g\beta B_0$. Our experimental results of viscosity dependence on P_n in Figure 7 strongly support that the exchange interaction in a radical–triplet pair is very strong.

Solvent Polarity Effect on Net RTPM Polarization. It is interesting to discuss the solvent effect on the magnitude of the net polarization observed in TEMPO. Goudsmit et al.¹⁴ measured the P_n values in the BP–TEMPO system in 1,2-

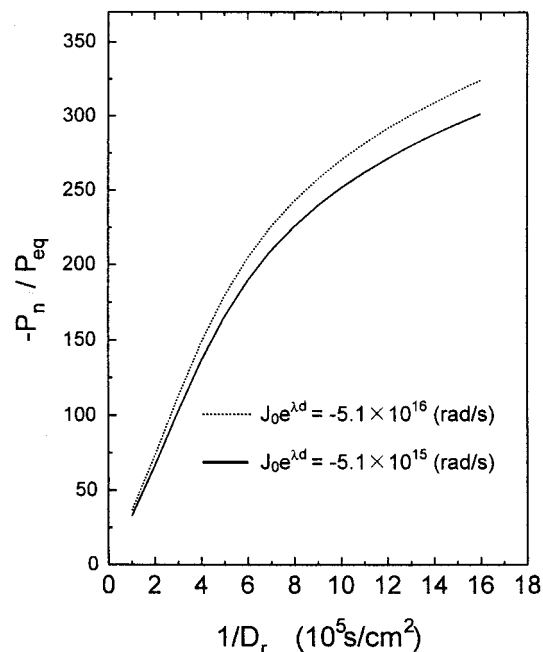


Figure 9. Effect of exchange interaction (J_0) on the magnitudes of net RTPM polarization calculated with the numerical analysis of SLE in eq 13 in the 1-chloronaphthalene–TEMPO system.

epoxypropane solution and obtained that $P_n = -0.6 P_{eq}$ at $D_r = 5.86 \times 10^{-5} \text{ cm}^2 \text{ s}^{-1}$. This magnitude is about 10 times smaller than our experimental result of $-6.9 P_{eq}$ obtained in benzene, although the diffusion coefficients are almost the same in both solvents at room temperature. This difference may be caused by the solvent effect on the J_0 value; the solvent polarity would affect the potential energy of the radical–triplet pair in Figure 1. Porter et al.² proposed that the contribution of CT interaction became more important in the triplet quenching by nitroxyl radicals with an increase in the triplet energy. The CT state in the BP–TEMPO system ($BP^{\cdot-} \cdots TEMPO^+$), which lies higher than the excited triplet state, will be stabilized in polar solvents such as 1,2-epoxypropane and might perturb the potential surfaces of the radical–triplet pair in Figure 1. This perturbation might make the energy splitting between the quartet and doublet states ($-3J_0$ in Figure 1) small. On the contrary, in nonpolar solvents such as benzene, the perturbation from the CT state would be much weaker, and thus, the quenching process will be dominated by the exchange interaction.¹⁷ Experiments about the solvent dielectric constant effect on the magnitude of net polarization are needed in the BP–TEMPO system. However, at least in benzene, our experimental result suggests that the quenching of the excited triplet state of BP by TEMPO proceeds via the exchange interaction. Contrary to the BP system, the magnitude of the exchange interaction was not apparently affected by the solvent polarity in the 1CN–TEMPO system; the J_0 value was estimated to be the same order of magnitude in both benzene and 2-propanol solutions. Even if the CT state is stabilized by the polar solvent molecules, the potential surfaces of the radical–triplet pair will not be perturbed by the CT state. This is caused by the fact that the free energy difference between the CT and the excited triplet states should be larger in the 1CN–TEMPO system than that in the BP–TEMPO system due to (1) lower energy of the excited triplet state of 1CN (2.57 eV) than that of BP (3.00 eV)^{2,24} and (2) lower reduction potential of 1CN (ca. -2.5 V vs SCE in N,N -dimethylformamide) than that of BP (-1.55 V).²⁴

Our results of large exchange interactions in radical–triplet pairs are consistent with the results reported in the laser flash

photolysis studies.^{3,4} Kuzmin et al.³ measured the quenching rate constants of the aromatic molecules by nitroxyl radicals in several solvents. They concluded that the quenching proceeded via energy transfer with the electron exchange interaction rather than enhanced intersystem crossing with charge-transfer interaction due to no solvent polarity dependence on the quenching rate constants by nitroxyl radicals. Considering that the quenching of triplet molecules by TEMPO in Table 1 occurs at a rate close to the diffusion limit, the exchange interaction in the excited triplet molecule–TEMPO system should be the same order of magnitude as that in the transient radical pairs. Therefore, the exchange interaction in a radical–triplet pair estimated above is reasonable. To completely clarify the mechanism of the quenching process of the excited molecules by radicals, more experiments on the magnitudes of net polarization seem to be needed in many molecular systems and in several solvents. However, our experimental results strongly suggest that the exchange interaction in the excited triplet molecule–TEMPO systems is strong and that the triplet molecules are quenched by TEMPO with energy transfer through the electron exchange mechanism.

6. Conclusion

We have quantitatively measured the absolute magnitudes of net CIDEP generated through the quenching of the excited triplet 1-chloronaphthalene, benzophenone, and benzil by TEMPO radical in benzene. In the 1-chloronaphthalene–TEMPO system, viscosity dependence on the polarization was also investigated in 2-propanol. We have proposed a theoretical treatment for the net CIDEP generation in the system of quartet–doublet spin states resulting from the radical–triplet molecule interaction with strong exchange interaction. According to this treatment, the spin polarization is effectively generated through the zero-field splitting interaction in the level-crossing region. Obtained magnitudes of net spin polarization are well explained with the theory. Numerical analysis based on our proposed theory has perfectly reproduced the viscosity dependence on the magnitude of polarization and clearly demonstrated for the first time that the magnitude of polarization exceeds $300 P_{\text{eq}}$ and that the back-transition from doublet to quartet states simultaneously occurs under viscous conditions ($\eta > 20$ cP). It has been demonstrated that the exchange interaction in a radical–triplet pair is much larger than the Zeeman energy of the X-band region (0.3 cm^{-1}).

We have also demonstrated that the electron exchange interaction in the system of an excited molecule and a free radical can be directly estimated from the magnitude of electron spin polarization caused by the radical–triplet pair mechanism.

Acknowledgment. We thank Dr. Yoshinari Konishi (National Industrial Research Institute of Nagoya) for his support of the methods of numerical analysis of SLE, and Prof. Shozo

Tero-Kubota (Institute for Chemical Reaction Science, Tohoku University) for useful discussions. This research has been partially supported by a Grant-in-Aid on Priority-Area-Research “Photoreaction Dynamics” from the Ministry of Education, Science, Culture, and Sports, Japan (06239103).

References and Notes

- (1) Birks, J. B. *Photophysics of Aromatic Molecules*; Wiley-Interscience: New York, 1970.
- (2) Gijzemann, O. L. J.; Kaufmann, F.; Porter, G. *J. Chem. Soc., Faraday Trans. 2* **1973**, 69, 727.
- (3) Kuzmin, V. A.; Takikolov, A. S. *Chem. Phys. Lett.* **1977**, 51, 45; **1978**, 53, 606.
- (4) Watkins, A. R. *Chem. Phys. Lett.* **1980**, 70, 262.
- (5) Naqvi, K. R.; Wild, U. P. *Chem. Phys. Lett.* **1976**, 41, 570.
- (6) Watkins, A. R. *Chem. Phys. Lett.* **1974**, 29, 526.
- (7) Takikolov, A. S.; Levin, P. P.; Kokrashvilli, T. A.; Kuzmin, V. A. *Bull. Acad. Sci. USSR* **1983**, 3, 465.
- (8) Suzuki, T.; Obi, K. *Chem. Phys. Lett.* **1995**, 246, 130.
- (9) Imamura, T.; Onitsuka, O.; Obi, K. *J. Phys. Chem.* **1986**, 90, 6471.
- (10) Blättler, C.; Paul, J. F. *Chem. Phys. Lett.* **1990**, 166, 375.
- (11) Kawai, A.; Okutsu, T.; Obi, K. *J. Phys. Chem.* **1991**, 95, 9130.
- (12) Kawai, A.; Obi, K. *J. Phys. Chem.* **1992**, 96, 52; **1992**, 96, 5701.
- (13) Kawai, A.; Obi, K. *Res. Chem. Intermed.* **1993**, 19, 865.
- (14) Goudsmit, G. H.; Paul, H.; Shushin, A. I. *J. Phys. Chem.* **1993**, 97, 13243.
- (15) Goudsmit, G. H.; Paul, H. *Chem. Phys. Lett.* **1993**, 208, 73.
- (16) Kobori, Y.; Kawai, A.; Obi, K. *J. Phys. Chem.* **1994**, 98, 6425.
- (17) Kobori, Y.; Mitsui, M.; Kawai, A.; Obi, K. *Chem. Phys. Lett.* **1996**, 252, 355.
- (18) Shushin, A. I. *J. Chem. Phys.* **1992**, 97, 3171.
- (19) Shushin, A. I. *Chem. Phys. Lett.* **1993**, 208, 173.
- (20) Shushin, A. I. *J. Chem. Phys.* **1993**, 99, 8723.
- (21) Adrian, F. J. *Chem. Phys. Lett.* **1994**, 229, 465.
- (22) Murai, H.; Imamura, T.; Obi, K. *Chem. Phys. Lett.* **1982**, 87, 298.
- (23) Terazima, M.; Okamoto, K.; Hirota, N. *J. Phys. Chem.* **1993**, 97, 13387.
- (24) Murov, S. L. *Handbook of Photochemistry*; Marcel Dekker: New York, 1993.
- (25) Adrian, F. J. *Rev. Chem. Intermed.* **1979**, 3, 3. Müss, L. T.; Atkins, P. W.; McLauchlan, K. A.; Pedersen, J. B. *Chemically Induced Magnetic Polarization*; Reidel: Dordrecht, 1977.
- (26) Adrian, F. J.; Monchick, L. J. *Chem. Phys.* **1979**, 71, 6.
- (27) Buckley, C. D.; McLauchlan, K. A. *Chem. Phys. Lett.* **1987**, 137, 91.
- (28) Blättler, C.; Paul, J. F. *Res. Chem. Intermed.* **1991**, 16, 201.
- (29) Terazima, M.; Hirota, N.; Shinohara, H.; Saito, Y. *J. Phys. Chem.* **1991**, 95, 9080.
- (30) Wasielewski, M. R.; O’Neil, M. P.; Lykke, K. R.; Pellin, M. J.; Gruten, D. M. *J. Am. Chem. Soc.* **1991**, 113, 2774.
- (31) Lane, P. A.; Swanson, L. S.; Ni, Q.-X.; Shinar, J.; Engel, J. P.; Barton, T. J.; Jones, L. *Phys. Rev. Lett.* **1992**, 68, 887.
- (32) Bennati, M.; Grupp, A.; Mehring, M.; Dince, K. P.; Fink, J. *Chem. Phys. Lett.* **1992**, 200, 440.
- (33) Turro, N. J.; Koptuyug, I. V.; Willingen, H. V.; McLauchlan, K. A. *J. Magn. Reson. A* **1994**, 109, 121.
- (34) Paul, H. *Chem. Phys.* **1979**, 40, 265.
- (35) Tominaga, K.; Yamauchi, S.; Hirota, N. *J. Chem. Phys.* **1988**, 88, 553.
- (36) Shushin, A. I. *Chem. Phys.* **1990**, 144, 223.
- (37) McLauchlan, K. A. *Modern Pulsed and Continuous-Wave Electron Spin Resonance*; John Wiley & Sons: New York, 1990.
- (38) Avdievich, N. I.; Forbes, M. D. E. *J. Phys. Chem.* **1996**, 100, 1993.
- (39) Batchelor, S. N.; Heikkilä, H.; Kay, C. W. M.; McLauchlan, K. A.; Shkrob, I. A. *Chem. Phys.* **1992**, 162, 29.
- (40) Verma, N. C.; Fessenden, R. W. *J. Chem. Phys.* **1976**, 65, 2135.